DCT-based local motion blur detection

Conference Paper · December 2009

DOI: 10.1109/ICICI-BME.2009.5417252 · Source: IEEE Xplore

3 authors:

E. Kalalembang
Institut Teknologi Telkom

Koredianto Usman
Telkom University

Irwan Prasetya Gunawan
Universitas Bakrie

DCT-based Local Motion Blur Detection

Erik Kalalembang[1], Koredianto Usman[1], Irwan Prasetya Gunawan[2]
[1]Departemen Teknik Elektro, Jurusan Teknik Telekomunikasi, Institut Teknologi Telkom
Jl. Telekomunikasi Dayeuhkolot, Bandung 40275 Indonesia
[2]Center for New Media ICT Research, Universitas Multimedia Nusantara
Scientia Garden, Gading Serpong, Indonesia
[1]erik_kalalembang@yahoo.com, [1]kru@ittelkom.ac.id, [2]irwan@unimedia.ac.id

Abstract – One of the frequently encountered problems in photography is the appearance of motion blurring effect due to either object movement or camera motion associated with the speed of the camera (shutter speed) when pictures are taken. This Paper presents a novel but simple method of detecting unwanted motion blur effects that appear local within an arbitrary area on a digital image. The proposed method uses various size block-based discrete cosine transform (DCT) calculations on the distorted image. The outcome of this detection are then subsequently used to improve the quality of the image by means of pixel correlation based deblurring method applied to the specific area identified by our motion blur detector. Subjective experiment to evaluate the quality of the resulting enhanced image is then conducted and objective evaluations using several published image quality metrics are also computed. Experimental results show that the quality of the enhanced images produced by the chosen deblurring method is better when local motion blur detection is employed than those without blur detection. Out of various block sizes used in the experiment, block size of 32 x 32 pixels produce better perceived quality.

Keyword: motion blur, deblurring, Discrete Cosine Transform, pixel correlation.

I. INTRODUCTION

Blurring efect is a very common distortion artifact in the photography field. Blur could come up due to various reasons, including out-of-focus camera lens, very extreme light intensity, lenses physical imperfection causing optical deviation, and relative movement of the object with respect to the camera lens. The latter are known to cause motion blur distortion in which the details of the object captured on the image have shifted in position resulting in an unclear appearance of both the texture and edges of the object. Motion blur could also be produced un-intentionally by imperfect digital image capturing process when the capturing device is in slight motion during the acquisition. On the other hand, motion blur effects may deliberately be introduced to create a sense of fast movement of the object and photographers use this to produce dramatic effect to the picture taken for more image appeal.

Some examples of motion blur effect on picture are illustrated in Fig. 1. Motion blurring in Fig. 1(a) is an example when the effect may be desired by the photographer; the effect is created by choosing slower shutter speed camera settings Fig. 1compared to the object's movement. The blur distortion in Fig. 1(b) is, on the other hand, may be unwanted since it has rendered the picture unclear. This unwanted effect may appear as a result of imperfect image scanning or camera shake. Notice how the global motion blur in Fig. 1(b) is different from the local motion blur in Fig. 1(c) where distortion appears only at some regions on the picture. The perceived quality of these two pictures, however, may not be that far.

Quality enhancement of global blur distorted pictures has been reported in [1] where pixel correlation method is proposed to mitigate both the gaussian and motion blur. Unfortunately, since the method works globally on the image, it may be sometimes counter productive because every areas on the picture are subjected to the procedure. This unnecessary handling of clear areas (ie, those where distortion is absence) should be avoided. Our proposed method presented in this Paper aims at improving the method of [1] by detecting local motion blur on the picture. The result of this detection is used as a basis for selecting the distorted areas for further processing (eg, deblurring, for example).

The rest of the paper is organised as follows. In Section II, we will review some theoretical backgrounds and previous

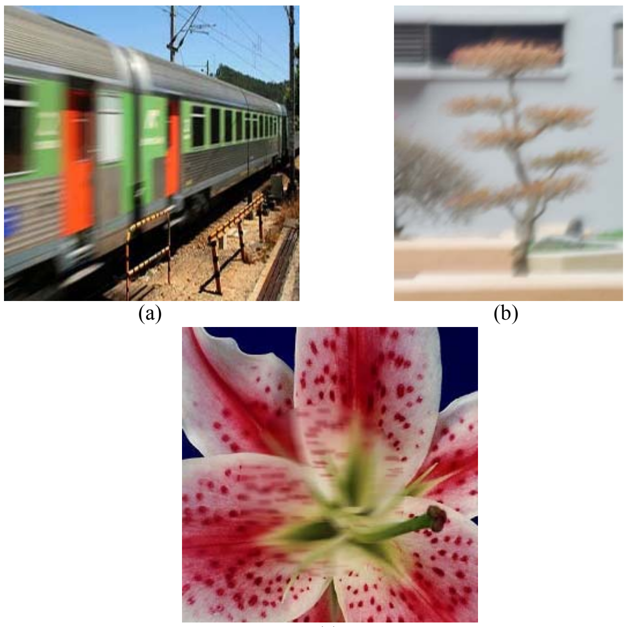

(a) (b) (c)

Fig. 1. Some examples of different motion blur effects on picture:
(a) deliberate/desired motion blur to create a sense of fast movement;
(b) unwanted motion blur on the whole image; (c) unwanted local motion blur.

works related to ours. Our proposed method is described in Section III, whilst the results of our experiments and its analyses will be given in Section IV. We conclude the paper with some conclusions in Section V.

II. BACKGROUND

A. Blur artifact

Blurring is reduced sharpness of edges and spatial details [2]. It can be modelled as a shifting towards lower frequencies component on the frequency domain. It may also be introduced by applying low pass filter to the image when high frequency components are filtered out [3]. Considered as distortion, it might happen as a result of an imperfect image acquisition process such as uniform linear motion between the image and the sensor [4]. In a compressed image, blurring is typically found in low bit rates JPEG/MPEG compressed image/video, particularly when coarse quantization is used [5].

Motion blur on digital image can be modeled as a convolution between the image and the motion blur kernel having point spread factor (PSF) distribution equals to the angle of the blur [1]:

$$\mathrm{H}(x,y) = f^{\alpha} * m = \sum_{K=0}^{K=1} m_{\mathrm{K}}\, f(x + K\cos\alpha\,, y + K\sin\alpha) \qquad (1)$$

with K and α is the coefficient and the direction of shifting angle, respectively. An example of motion blur kernel with blur length of 7 and angle of 45^{o} is shown in Fig. 2.

Blurring distortion can be detected through several different methods. Methods in [6] and [7] work in spatial domain and effective for gaussian blur. Methods working in frequency domain based on Fourier transform are also available [8; 9], but these methods require some sort of references (which can be full frame picture or its reduced form) for successful operation and are more focus on the quality assesment of image/video sequence rather than blur detection. Blur detection of [6] requires no reference at all, but in addition of working in the spatial (pixel) domain, it is also a global blur metric. More complicated methods based on PSF estimation have been reported by many; see a detailed review of such methods in [10]. The main drawback of these methods is its complexity which can hinder their use for practical applications.

A more logical approach to this problem is to use DCT coefficients for estimating the amount of blur. The rationale of this approach is the availability of such DCT coefficients from today's abundant images which are already in compressed form. The DCT coefficients of JPEG compressed images are deeply related to the image content. The methods proposed by [11] and [12] follow this idea. Their methods based on extracting DCT coefficients from the compressed image or MPEG bitstream. However, their approaches have several drawbacks [12]: first, the method by [11] requires DCT computation on the largest possible set of data, ideally on the whole image (for example, an image of size 256 x 256 pixels must be transformed into a 256 x 256 DCT matrix). Second, in addition to that, this method involves a lot of computation to manipulate DCT coefficients and detect some absolute minima. Third, the method by [12] depends on the classical 8x8 DCT blocks. Unfortunately, today's advanced encoding based on H264/AVC uses various block sizes, which obviously limits the applicability of this method. This method also uses histograms of non-zero DCT occurrences, computed directly from MPEG/JPEG compressed images. Since it is used to measure image quality, the blur is characterized globally. Last but not least, since this method relies on extracting the DCT coefficients from the compressed domain, it implies that the image should be in compressed format, which may not be applicable for some applications.

0	0	0	0	0	0.0145	0
0	0	0	0	0.0376	0.1283	0.0145
0	0	0	0.0376	0.1283	0.0376	0
0	0	0.0376	0.1283	0.0376	0	0
0	0.0376	0.1283	0.0376	0	0	0
0.0145	0.1283	0.0376	0	0	0	0
0	0.0145	0	0	0	0	0

Fig. 2. Motion blur kernel with blur length = 7 and angle = 45°

B. Discrete Cosine Transform

Discrete cosine transform (DCT) coefficients of an image reflect the frequency distribution of an image [12]. It also posses compaction property by which image information may be distributed across as few transform coefficients as possible. On a digital image, the two-dimensional version of DCT can be computed as:

$$B_{pq} = \alpha_p \alpha_q \sum_{m=0}^{M-1}\sum_{n=0}^{N-1} A_{mn} \cos\frac{\pi(2m+1)p}{2M} \cos\frac{\pi(2n+1)q}{2N} \qquad \begin{matrix} 0 \le p \le M-1 \\ 0 \le q \le N-1 \end{matrix} \qquad (2)$$

$$\alpha_p = \begin{cases} 1/\sqrt{M} & ,p = 0 \\ \sqrt{2/M} & ,1 \le p \le M-1 \end{cases}$$

$$\alpha_q = \begin{cases} 1/\sqrt{N} & ,q = 0 \\ \sqrt{2/N} & ,1 \le p \le N-1 \end{cases}$$

where A is the input matrix of size N x M, and B_{pq} is the DCT coefficients of A. The input matrix A can be chosen as full image; but in principle, this matrix can also be chosen from any subset areas on the image. For practical reasons, the size of input matrix A is usually chosen as power of 2.

DCT is reversible transform. The inverse DCT can be computed as:

$$A_{mn} = \alpha_p \alpha_q \sum_{m=0}^{M-1}\sum_{n=0}^{N-1} \alpha_p \alpha_q\, B_{pq} \cos\frac{\pi(2m+1)p}{2M} \cos\frac{\pi(2n+1)q}{2N} \qquad \begin{matrix} 0 \le p \le M-1 \\ 0 \le q \le N-1 \end{matrix} \qquad (3)$$

$$\alpha_p = \begin{cases} 1/\sqrt{M} & ,p = 0 \\ \sqrt{2/M} & ,1 \le p \le M-1 \end{cases}$$

$$\alpha_q = \begin{cases} 1/\sqrt{N} & ,q = 0 \\ \sqrt{2/N} & ,1 \le p \le N-1 \end{cases}$$

The least equation implies that the output image can be regarded as a linear combination of the following DCT basis functions:

$$\alpha_p \alpha_q \cos\frac{\pi(2m+1)p}{2M} \cos\frac{\pi(2n+1)q}{2N} \qquad \begin{matrix} 0 \le p \le M-1 \\ 0 \le q \le N-1 \end{matrix} \qquad (4)$$

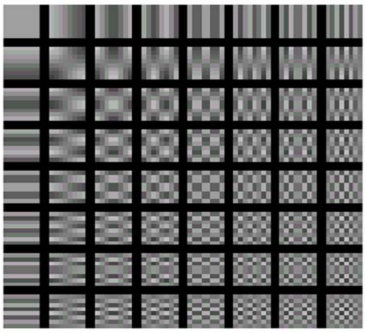

Fig. 3. DCT basis functions for 8x8 matrix

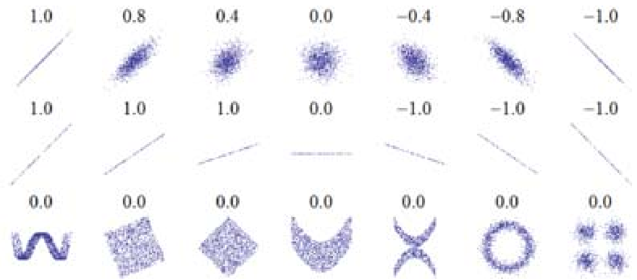

Fig. 4. Correlation coefficients of various patterns [1]

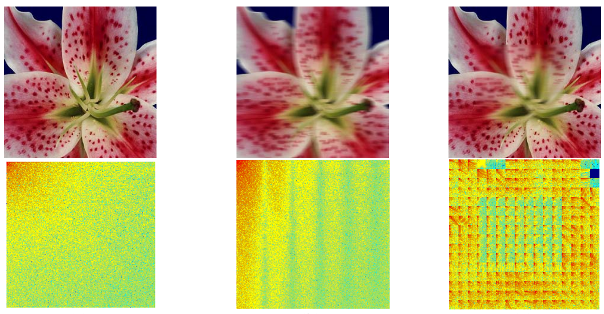

(a) (b) (c)

Fig. 5. Images with different amount of motion blur and their corresponding DCT coefficients: (a) no blur with DCT computed on the whole image; (b) global motion blur with DCT computed on the whole image; (c) local motion blur with DCT computed on a block-by-block basis of 8x8 pixel.

From (2), (3), and (4), it is clear that B_{pq} acts as a weighting coefficient for each DCT basis function. For a coefficient matrix of size 8x8, the basis function is illustrated in Fig. 3. Different matrix size would produce different basis functions from Fig. 3.

C. Pixel correlation for deblurring image

Correlation shows a linear association between two random variables. It is computed by pairing the two variables and calculate their product-moment coefficient. Correlation values may range from -1 to 1. The sign of the values implies the ‘direction’ of the association; e.g., negative correlation means that relatively high values on one variable are paired with relatively low scores on the other variable, and vice versa for positive correlation. Weak agreement between the two random variables is shown by correlation values close to zero.

Pixel correlation on a 2D image is illustrated in Fig. 4. It can be seeen that correlation values are related to the angle/direction of the pixels and the nature of the data [1]. Correlation between pixels depends on the slope of the data, the linear (or non-linear) trends between them, and the degree of noise that contains in it.

On motion blurred images, pixel correlations can be used to estimate the amount of angle and pixel shifts; i.e., the kernel of the motion blur. Based on this estimated kernel, image enchancement through deblurring process [1] can be performed.

III. Method

A. Overview

Our motion blur detection method relies on the observation that motion blur shifts the frequency content of the blurred areas into lower frequency components, such as explained in Section II.A. In terms of its DCT coefficients distribution, motion blur can be marked as areas on image where higher frequency DCT coefficients are more significant in number than the lower frequency components, but at the same time showing much less energy than on image without blur.

This basic idea is illustrated in Fig. 5. Three images with different amount of motion blur giving rise to various DCT coefficient distributions are depicted in this figure. Image having no blur distortion (Fig. 5(a)) shows a typical distribution on the DCT domain; i.e., some energy is stored on lower frequency components whilst some other is distributed amongst higher frequency components albeit with less strength (amplitude). Note that although these higher frequency components bear lower amplitudes than their lower frequency counterpart, higher frequency components are responsible for image texture, spatial details, and general sharpness of the image. Changes in the frequency content of the image are imminent when global blur is introduced (Fig. 5(b)); higher frequency components are more supressed whilst lower frequency components are enhanced dramatically. Note also that since the global blur injected to the image is of motion type bearing certain direction, this is reflected in the DCT content of the image itself. However, although global DCT computation such as this example shows some promises in detecting global motion blur, nothing is said much about the location where motion blur occur. Recall our earlier illustration on Fig. 1(a) where motions blur only appears on some parts of the image (partial blur). Global DCT computation does not give any useful information here. Instead of using global DCT computation, we use DCT computed on smaller block size on many areas on the image and examine the results of each computation. This is exactly what we show in Fig. 5(c). By performing local DCT computation, motion blurred areas and their location can be detected.

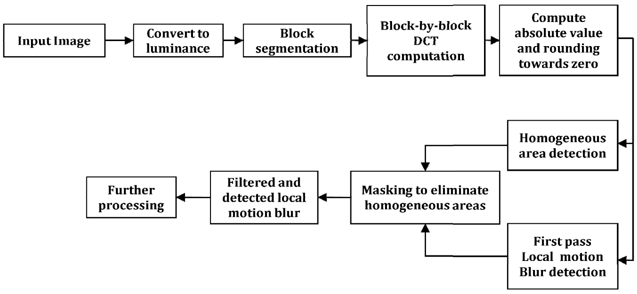

Fig. 6. Proposed local motion blur detection

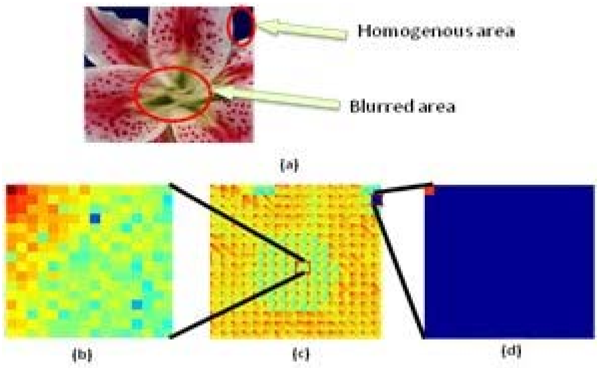

Fig. 7. DCT coefficient profile for different areas on image: (a) image containing blurred as well homogeneous areas; the local, block-by-block DCT coefficients are shown in (c). Block DCT of blurred and homogenous areas are depicted in (b) and (d), respectively.

B. Local motion blur detection

Based on the observation we have explained in the previous section, we developed our local motion blur detection method as depicted in Fig. 6. First, the partially motion-blurred image is converted into luminance image prior to DCT computation. This conversion is used since we do not really need colour information to detect blurred areas from DCT coefficients. We compute these coefficients on each partitioned blocks, take their absolute values, and then round them towards zero. Various block sizes are used: 8x8, 16x16, 32x32, and 64x64 pixels.

The subsequent process involves two separate computations. First, we identify areas with significantly low amplitude of higher frequency components to mark them as potential candidate for blurred areas. However, since flat regions such as blocks containing no edge structures as well low-contrast regions also exhibit similar characteristics, such simple identification may not be reliable enough to distinguish blurred areas from homogeneous areas (flat or low-contrast regions). This problems is reported by [13] and had caused errors in their detection method resulting in low, unsatisfactory performance in terms of its accuracy rate. We propose to mitigate such problem by introducing second computation to identify homogeneous areas through each blocks' standard deviation. Areas with low standard deviation are marked as homogeneous areas. This is illustrated in Fig. 7.

Note that a block may be identified as both potentially blurred area (due to low amplitude of higher frequency components) and homogenous area (due to low standard deviation). If this is the case, then we have to ignore this block and count it as non-blur area. We implement this by means of a masking process to eliminate homogeneous areas from the potentially blurred areas. The result of this masking operation is a collection of areas on image where motion blur really occurs.

C. Deblurring

Once the areas where motion blur appears have been identified by our method described in Fig. 6, selective deblurring through pixel correlation method can be performed. We use the deblurring method presented in [1] for this purpose.

D. Evaluation

Evaluation to the proposed method are performed through objective and subjective assessments. We compare the quality of the resulting deblurred images with the input to observe how much improvement have been injected to the input to increase the quality of the final images.

Several objective assessment methods are chosen for our experiments; i.e. methods based on structural similarity [14], correlation and contrast similarity [15], and block activity [16]. The first two assessment methods are relative metric with respect to a reference image. Usually, this reference is taken from the original image having no distortion. However, since in our experiment the original image is unknown, we use the input image (i.e. the partially motion blurred image) as reference. In this way, we measure how much different is the (partially) deblurred image compared to this input. The structural similarity between the recovered deblurred areas and the motion blurred areas should be moderately low to indicate that these areas have been properly identified by our proposed method and have subsequently gone through the selective deblurring process. When the deblurring process fails (e.g. no areas are selected by our method hence no deblurring), the final output of the image would be very similar to the input, resulting in a very high similarity index. On the other hand, when deblurring process is applied to all areas regardless whether these areas contain motion blur artefacts or not, we can expect that in general the final image is completely different from the input, resulting in a significantly low similarity index.

The third objective metric we have chosen to assess our method is based on block activity on image. The activity is measured using two factors: the average absolute difference between in-block image samples, and the zero-crossing rate of the pixels [16].

We also perform subjective experiments in which viewers are asked to rate the quality of the deblurred images using several different settings on our method (i.e. different block sizes, different standard deviation values). Subjective experiments data were collected from 30 observers. The MOS (mean opinion score) are then compiled and averaged for all images.

IV. Results and Discussions

A. Experiments on block size

The results of our experiments using various block size are given in Fig. 8. We can see that smaller block size (i.e. 8x8) results in finer detail of detection, but in some images also exhibit less accuracy; i.e. there are false detections of local motion blur in addition to the method failing to detect blurred area at all. Large block size (i.e. 64x64) produces smaller resolution of detection; e.g. the detected blurred areas are smaller than the actual ones.

Fairly best results were produced by moderate block size; e.g. 16x16 pixels. By using this block size, the sizes of the detected blurred areas are very close to the actual ones.

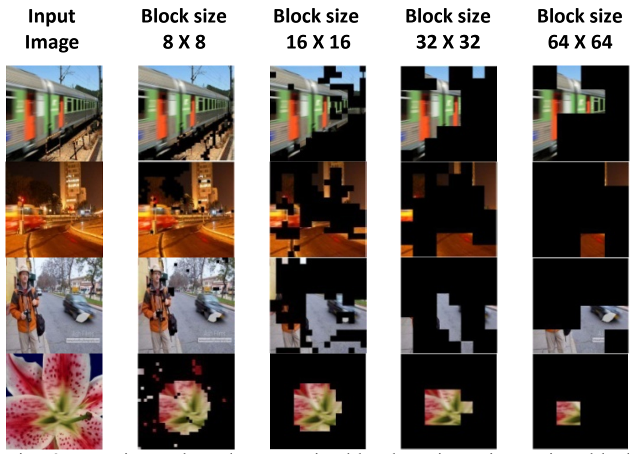

Fig. 8. Experimental results on motion blur detection using various block sizes with block standard deviation threshold of 25.

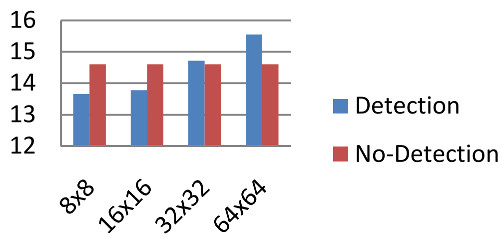

Fig. 9. No-reference image quality metrics based on [16] on image with local motion blur detection (our method) and no-detection/global deblurring of [1].

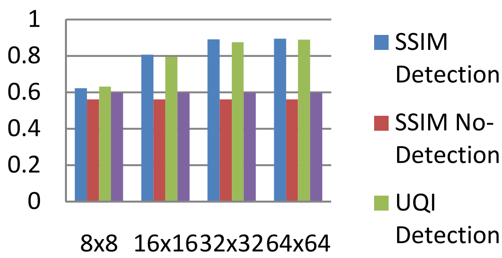

Fig. 10. SSIM and UQI-based image assessment for various block size, both for methods with local motion blur detection (ours) and no-detection/global deblurring of [1].

B. Objective assessment

Block activity-based objective metric index for standard deviation threshold of 25 is given in Fig. 9. No-reference image quality metrics based on on image with local motion blur detection (our method) and no-detection/global deblurring of . On the other hand, similarity-based metric of the deblurred images resulting from a series of experiments involving local motion blur detection followed by deblurring method is given in Fig. 10.

Fig. 9 shows that the index of the deblurred images with our local detection method is larger than that of the deblurred images without detection method for block size larger than 32x32. This result suggests that selecting the appropriate block size for local detection method could further improve the quality of the resulting deblurred image compared to a method that globally deblur the image without any selection criteria for detecting motion blur on image.

Fig. 10 demonstrates a comparison between SSIM and UQI-based indices for deblurred images with our local detection method and that without detection such as implemented in [1]. In general, applying deblurring method at all areas on image containing only local motion blur distortions would further degrade the quality of the image. Our selection method, on the other hand, is able to identify which areas on image should be further processed with deblurring method and leave the rest untouched. Therefore, whilst the blurred areas are modified and reconstructed by the deblurring method (and consequently would exhibit different image structure from the blurred areas) contributing to the lower value of SSIM/UQI indices on that *particular* part of the image, the clear areas on image still bear very close (or even identical) structure to those of the input image contributing to higher value of SSIM/UQI indices. The total index would be something that is moderately low enough (or moderately high, depending on perspective) to separate them from the index of deblurred images without any detection.

Notice that the less accurate characteristics of ours using smaller block size (e.g. 8x8 pixels) such as illustrated in Fig. 8 is confirmed by the objective assessments given in Fig. 9 and Fig. 10; this block size shows very poor performance in terms of block activity-based metric and SSIM/UQI indices.

C. Subjective assessment

The results of our subjective evaluation are given in Fig. 11. This graph supports the data we have presented before; i.e. better perceived quality of deblurred images pre-processed by our local motion blur detection method is achieved when moderately large block size (e.g. 32x32 pixels) is chosen.

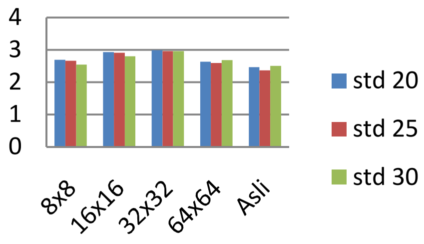

Fig. 11. Averaged MOS data from 30 observers for deblurred images and input (original) image

V. Conclusions

We have shown from our experimental results that our method of local motion blur detection could further increase the performance of deblurring method. For images contaminated with local motion blur artefacts, our method outperforms the other that performs deblurring process globally at all areas on image. An appropriate selection of block size for the detection is necessary; too small of block size would result in false detection of blurred areas or failed altogether. Objective assessments of our method have also been supported by subjective evaluation.

References

1. **Imbar, Gusfrian, Usman, Koredianto and Hidayat, Bambang.** *Desain dan Implementasi Image Debluring Menggunakan Metode Korelasi Koefisian dan Lucy Richardson.* Bandung : Institut Teknologi Telkom, 2008.
2. **Yuen, M and Wu, H.** A survey of hybrid MC/DPCM/DCT video coding distortions. *Signal Processing.* 1998, Vol. 70, pp. 247-278.
3. **Farias, M, Mitra, S K and Foley, J M.** Perceptual Contributions of Blocky, Blurry and Noisy artifacts to overall annoyance. *Proc. ICME.* 2003, Vol. I, pp. I-529-32.
4. **Gonzales, R C and Woods, R E.** *Digital Image Processing.* 2nd Ed. Upper Saddle River : Prentice-Hall, 2002.
5. **Zhang, X and Wandell, B A.** Color Image Fidelity Metrics Evaluated using Image Distortion Maps. *Signal Processing.* November 30, 1998, Vol. 70, 3, pp. 201-214.
6. **Marziliano, P, et al.** A No-Reference Perceptual Blur Metric. *Proc. ICIP (IEEE International Conference on Image Processing).* 2002, Vol. 3, pp. 57-60.
7. **Dijk, J, et al.** A New Sharpness Measure Based on Gaussian Lines and Edges. *Proc. Int. Conf. CAIP.* 2003, Vol. 2756, hal. 149-156.
8. **Gunawan, Irwan Prasetya and Ghanbari, Mohammed.** Reduced-Reference Video Quality Assessment using Discriminative Local Harmonic Strength with Motion Consideration. *IEEE Trans. Circuit and Systems for Video Technology.* January 2008, Vol. 18, 1, pp. 71-83.
9. **Tan, Kwee Teck and Ghanbari, Mohammed.** A Multimetric Objective Picture Quality Measurement Model for MPEG Video. *IEEE Trans. Circuit and Systems for Video Technology.* October 2000, Vol. 10, 7, pp. 1208-1213.
10. **Nayar, S. K. and Ben-Ezra, M.** Motion-based motion deblurring. *IEEE Trans. Pattern Analysis and Machine Intelligence.* June 2004, Vol. 26, 6, pp. 689-698.
11. **Yoshida, Y., Horiike, K. dan Fujita, K.** Parameter Estimation of Uniform Image Blur Using DCT. *IEICE Trans. Fundamentals.* July 1993, Vol. E76, 7, hal. 1154-1157.
12. **Marichal, X, Ma, Wei-Ying and Zhang, HongJiang.** Blur determination in the compressed domain using DCT information. *Proc. ICIP (IEEE International Conference on Image Processing).* 1999, Vol. 2, pp. 386-390.
13. **Liu, Renting, Li, Zhaorong dan Jia, Jiaya.** Image Partial Blur Detection and Classification. *CVPR.* 2008.
14. **Wang, Zhou, et al.** Image Quality Assessment: From Error Visibility to Structural Similarity. *IEEE Trans. on Image Processing.* April 2004, Vol. 13, 4, hal. 600-612.
15. **Wang, Zhou dan Bovik, Alan Conrad.** A Universal Image Quality Index. *IEEE Signal Processing Letters.* March 2002, Vol. 9, hal. 81-84.
16. **Wang, Zhou, Seikh, Hamid Rahim dan Bovik, Alan Conrad.** No-reference perceptual quality assessment of JPEG compressed images. *Proc. ICIP.* 2002.